Combined ADRC and Model Reference-Based Input Filter for Overhead Crane Control: Design and Experimental Validation

Trong Hieu Do
School of Electrical and Electronic Engineering
Hanoi University of Science and Technology
Vietnam

Overhead cranes are widely used in industry and transportation, but their operation is often affected by undesired payload oscillations that degrade maneuverability and safety. Although numerous control strategies have been investigated, most of them are relatively complex in both controller design and practical implementation. This paper proposes a hybrid control scheme that integrates Active Disturbance Rejection Control (ADRC) with a model reference-based input filter, where ADRC ensures accurate trolley positioning and the filter suppresses payload swings .reducing the need for precise system modeling and mitigating the impact of parameter uncertainties. Simulation results confirm that the proposed approach effectively eliminates payload oscillations while achieving the desired positioning, and experimental validations further demonstrate its robustness and practical feasibility for crane operations.

Keywords: *Overhead crane, vibration control, ADRC; Model reference; Output-based filter;*

1. INTRODUCTION

Overhead cranes are indispensable transportation devi–ces widely employed in various industrial sectors, inc–luding manufacturing, logistics, and construction, where the handling of heavy loads exceeds human capability. Their primary functions involve transporting, lifting, and lowering goods or equipment with high precision and efficiency. However, due to their characteristics, overhead cranes can be modeled as pendulum-like systems in which the payload is suspended from the trolley via a flexible cable. As a result, the payload is indirectly actuated, rendering the system under actuated with more degrees of freedom than available control inputs [1]. Furthermore, variations in payload mass and rope length, arising from operational requirements, introduce uncertainties that further challenge control design. Without effective vibration suppression, unde–sired oscillations may occur during transportation, degrading positioning accuracy, increasing operation time, and potentially compromising safety. Consequ–ently, the design of robust and efficient control stra–tegies for overhead cranes has attracted substantial research attention over the past decades and continues to remain a critical issue [2].

Numerous studies have addressed the control prob–lem of overhead crane systems, giving rise to a broad spectrum of control strategies. In [3-5], the authors developed PID controllers to suppress payload oscil–lations. For the nonlinear model, sliding mode control has been employed [6,7]. Other feedback control stra–tegies have been introduced for crane systems, such as PSO-based nonlinear feedback control [8], model pre–dictive control [9] and flatness theory [10], each contri–buting to enhanced positioning accuracy and improved system stability. Another advanced control approaches based on fuzzy logic models have attracted considerable attention, as reported in [11]. Nevertheless, the design and tuning of these controllers often demand substantial expertise from skilled engineers.Although numerous methods have shown effectiveness in controlling crane systems and suppressing load oscillations, achieving high-precision performance with feedback-based cont–rollers generally relies on multiple sensors to simul–taneously monitor trolley displacement and payload swing angles. The incorporation of these additional sen–sors not only increases system cost but also complicates the accurate measurement of payload oscillations. Such challenges primarily arise from variations in payload mass, geometry, and configuration, which can adversely affect sensor accuracy and ultimately compromise the overall reliability of the system. These challenges have motivated the exploration of alternative control stra–tegies that do not rely heavily on sensing infrastructure. In this regard, open-loop control systems have also been studied and applied in practice. One notable technique is input shaping, originally proposed by a research group at MIT, with its theoretical foundation presented in [12, 13]. The traditional input shaping method operates by generating a supplementary signal that cancels out the vibrations induced by the original input command. Among various open-loop control algorithms, input shaping has attracted significant attention and has been widely adopted in multiple applications, including over–head crane control [14,15], due to its simplicity, effec–tiveness, and practical feasibility. Nevertheless, most of existing studies have concentrated primarily on supp–ressing payload oscillations, while in practical applica–

Received: December 2025, Accepted: March 2026:
Correspondence to: Dr Trong Hieu Do
Hanoi University of Science and Technology,
No. 1 Dai Co Viet, Bach Mai, Hanoi, Vietnam
E-mail: hieu.dotrong@hust.edu.vn
doi: 10.5937/fme2602296H

tions, overhead cranes are also required to achieve high-precision positioning of loads at designated target locations.Therefore, this method is commonly combined with a position control loop for the trolley [16-19].

In this study, a hybrid control strategy is proposed that integrates Active Disturbance Rejection Control (ADRC) with a model reference-based input filter for overhead crane systems. To the best of our knowledge, this is the first attempt to combine ADRC with an output-based input filter in this application. ADRC is employed to ensure precise trolley positioning and actively compensate for external disturbances, while the input filter effectively suppresses payload oscillations using only system output signals. Since its introduction [20], ADRC has gained considerable attention as a promising alternative to traditional PID controllers. As a modern control metho–dology, it emphasizes real-time disturbance estimation and rejection without relying on an accurate mathematical model. Although ADRC has proven effective in enhancing disturbance rejection and adapting to load variations, residual vibrations may still arise due to the inherent dynamics of crane systems. To address this issue, combi–ning ADRC with a model reference-based input filter offers a promising solution. Proposed as an offline design method relying solely on system outputs [21], unlike traditional input shaping methods that rely on accurate knowledge of system dynamics, this filter seeks to minimize the difference between the actual system response and that of a reference model. It provides two main advantages: (a) requiring only system output signals, and (b) enabling the selection of suitable damping and bandwidth to achieve the desired dynamic performance. The proposed hybrid method is therefore designed to enhance ro–bustness against modeling uncertainties and external disturbances, while simultaneously reducing depen–dence on additional sensor instrumentation. By minimi–zing reliance on extra sensors, the approach lowers implementation cost and complexity, while improving practicality and reliability in crane operations.The main contributions of this paper are summarized as follows:

- A hybrid control framework is developed by integ–rating ADRC with a model reference-based input filter to achieve both precise trolley positioning and effective suppression of payload oscillations.
- The proposed approach minimizes dependence on accurate system modelling and additional sensors by exploiting only output signals in the filter design, thereby reducing cost and implementation complexity.

The remainder of this paper is structured as follows. Section 2 introduces the mathematical model of the overhead crane system along with the experiment setup. Section 3 describes the design of the proposed control strategy for position regulation and vibration suppres–sion. Section 4 presents simulation and experimental results, followed by the conclusions in Section 5.

2. OVERHEAD CRANE MODEL

2.1 Mathematical modelling

Consider the model of an overhead crane system mo–ving along the horizontal X- axis, with a payload suspended vertically along the Y-axis, as illustrated in Figure 1, where:

- x : position of the trolley
- l: length of the suspension cable
- θ : payload swing angle
- m_t : mass of the trolley
- m_p : mass of the payload

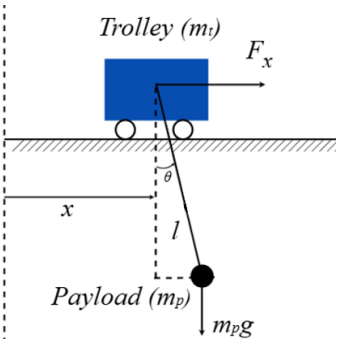

Figure 1. Model of a 2D overhead crane

Assuming that both the trolley and the payload are modeled as point masses, and that the cable's mass and elasticity are ignored. The position of the trolley (x_t, y_t) and the payload (x_p, y_p) in the XY-coordinate system is described as follows:

$$\begin{aligned}&(x_t, y_t) = (x, 0)\\&(x_p, y_p) = (x + l\sin\theta - l\cos\theta)\end{aligned} \tag{1}$$

The kinetic and potential energy of the entire system are calculated as follows:

$$T = T_{trolley} + T_{payload} = \frac{1}{2}m_t\dot{x}_t^2 + \frac{1}{2}m_p\left(\dot{x}_p^2 + \dot{y}_p^2\right) \tag{2}$$

The Lagrange function of the system is given by:

$$\begin{aligned}&L = T - P = \frac{1}{2}m_t\dot{x}^2 +\\&+\frac{1}{2}m_p\left(\dot{x}^2 + l^2 + l^2\dot{\theta}^2 + 2\dot{x}l\sin\theta + 2\dot{x}l\dot{\theta}\cos\theta\right) +\\&+m_p g l\cos\theta\end{aligned} \tag{3}$$

By applying the Lagrange method to the motion of the trolley along the X-axis and the rotational motion of the payload, we obtain:

$$\begin{aligned}&\left(m_t + m_p\right)\ddot{x} + m_p l\ddot{\theta}\cos\theta - m_p l\dot{\theta}^2\sin\theta +\\&+2m_p\dot{l}\dot{\theta}\cos\theta + m_p\ddot{l}\sin\theta = F_x - B_{eq}\dot{x}l\ddot{\theta} +\\&+\ddot{x}\cos\theta + g\sin\theta - B_p\dot{\theta}\end{aligned} \tag{4}$$

where $\boldsymbol{B_{eq}}$ isthe viscous damping coefficient of the trolley along the X-axis, $\boldsymbol{B_p}$ is therotational damping coefficient of the payload.

Assuming the rope length l is considered constant, i.e., $\dot{l} = \ddot{l} = 0$. Substituting these conditions into (4) and (5) yields the reduced system of equations describing the overhead crane model:

$$\begin{aligned}&\left(m_t + m_p\right)\ddot{x} + m_p l\ddot{\theta}\cos\theta - m_p l\dot{\theta}\sin\theta =\\&= F_x - B_{eq}\dot{x}l\ddot{\theta} + \ddot{x}\cos\theta + g\sin\theta = -B_p\dot{\theta}\end{aligned} \tag{5}$$

From (7), under the small-angle assumption where **cosθ** ≈ 1 and **sinθ** ≈ θ the transfer function relating the swing angle to the trolley position can be derived as follows:

$$\frac{\theta(s)}{X(s)} = \frac{-s^2}{ls^2 + B_p s + g} \tag{6}$$

2.2 Experimental model

To verify the proposed method in practice, an experimental 2D crane model in Figure 2 is considered. The experimental overhead crane comprises a trolley moves along the X−axis. A Mitsubishi HG-KN23J-S100 servo motor is used to control the X-axis of the overhead crane. When the trolley reaches the travel limit and triggers the limit switches, the model is automatically disconnected to ensure safety. The load of the system is designed as a single pendulum. It consists of a massattached to the hook, forming a simple pendu–lum that swings freely during the crane's movement. The oscillation angle of the load is measured using a rotary potentiometer, which provides continuous feed–back of the payload's angular displacement θ. In addi–tion, the trolley position x is obtained from the servo motor encoder. These measured signals are used for feedback control.

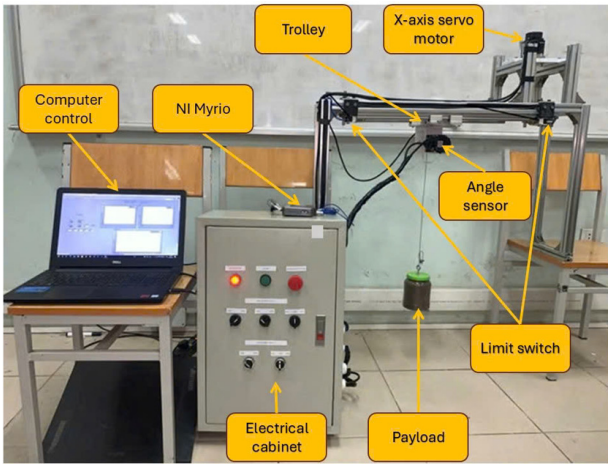

Figure 2. Model of a 2D overhead crane

The trolley motion is actuated through a servo motor and driver, which provide precise velocity regulation by varying the input control voltage. Consequently, the dynamic relationship between the control voltage input and the trolley position can be represented by the following transfer function [22]:

$$G_1 = \frac{X(s)}{U(s)} \tag{7}$$

Based on the system identification procedure, the dynamic relationship between the input voltage and the trolley position is represented by:

$$G_1 = \frac{6.26}{s(0.069s + 1)} \tag{8}$$

Similar to the identification of the position transfer function, the transfer function relating the trolley position to the payload swing angle is derived from the measured position and swing angle data, and can be expressed as follows:

$$G_2(s) = \frac{\theta(s)}{X(s)} = \frac{-K_\theta s^2}{ls^2 + B_p s + g} = \frac{K_t s^2}{s^2 + 2\xi\omega_t + \omega_t^2} \tag{9}$$

$$\omega_t = \sqrt{g/l}, g = 9.81\left(m/s^2\right), m = 1(kg) \tag{10}$$

To guarantee safe and efficient load transportation, this study develops a control strategy that addresses the following operational requirements:

1. The trolley is required to travel from the initial position x_i to the target position x_d.
2. The payload swing must be effectively suppressed throughout the entire motion, with zero residual oscillation at the final position.

The subsequent section presents the proposed control approach formulated to enhance the dynamic performance of the overhead crane system

3. CONTROL STRATEGY

The control system designed here is intended to achieve two objectives: to move the trolley to the desired position and to suppress the swing angle excited by the trolley motion. Therefore, an active disturbance rejection control (ADRC) scheme is employed for trolley position regulation, while a model-based input shaping filter is integrated to mitigate the swing angle. The combined structure of ADRC and the input shaping filter is illustrated in Figure 3.

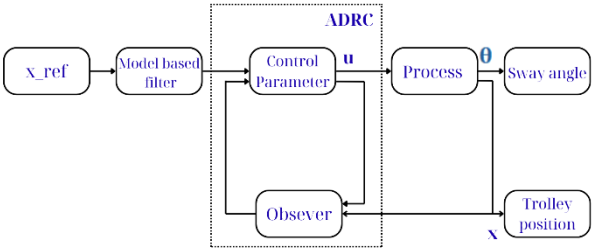

Figure 3. Control structure design

3.1 Trolley position control

In recent years, Active Disturbance Rejection Control (ADRC) has been recognized as an effective control methodology for addressing various challenges in dynamic systems [23, 24]. The ADRC framework comprises three fundamental components: an Extended State Observer (ESO) for estimating both the system states and the lumped disturbances; a linear feedback controller that regulates the control input to achieve fast and stable system responses; and a disturbance compensation mechanism that attenuates the impact of disturbances on the output. Owing to these features, ADRC is particularly suitable for nonlinear systems subjected to uncertainties and external disturbances, providing high accuracy and strong adaptability. Furthermore, ADRC has been reformulated into an industrially applicable structure, where controller design and implementation are greatly simplified through a parameter-tuning method based on the observer bandwidth, as reported in [25].

For trolley position control design base on ADRC, (10) can be rewritten as:

$$U(s) = Ts^2 X(s) + sX(s) \tag{11}$$

or in the time domain:

$$\ddot{x}(t) = (-1/T)\dot{x}(t) + (K/T)u(t) = f(t) + bu(t) \tag{12}$$

Generally, f comprise nonlinearities and parameter uncertainties, constituting a combined disturbance. The core idea of ADRC is the use of an Extended State Observer (ESO) to estimate the total disturbance term $\hat{f}(t)$, which allows the system to counteract the influence of $f(t)$ through disturbance rejection. For this purpose, equation (13) is reformulated in the state-space form as follows:

$$\begin{bmatrix} \dot{x}_t \\ \dot{x}_2(t) \\ \dot{x}_3(t) \end{bmatrix} = \underbrace{\begin{bmatrix} 0 & 1 & 0 \\ 0 & 0 & 1 \\ 0 & 0 & 0 \end{bmatrix}}_{A} \begin{bmatrix} x_1(t) \\ x_2(t) \\ x_3(t) \end{bmatrix} + \underbrace{\begin{bmatrix} 0 \\ b \\ 0 \end{bmatrix}}_{B} u(t) + \underbrace{\begin{bmatrix} 0 \\ 0 \\ 1 \end{bmatrix}}_{C} \dot{f}(t) \tag{13}$$

$$x(t) = \begin{bmatrix} 1 & 0 & 0 \end{bmatrix} \begin{bmatrix} x_1(t) \\ x_2(t) \\ x_3(t) \end{bmatrix} \tag{14}$$

The model of the extended state observer is cons–tructed as follows, with l_1, l_2, and l_3 as the parameters of the ESO, which are determined such that $\hat{z}_1, \hat{z}_2$, and $\hat{z}_3$ estimate x, $\dot{x}$, and f, respectively:

$$\begin{bmatrix} \hat{z}_1(t) \\ \hat{z}_2(t) \\ \hat{z}_3(t) \end{bmatrix} = \underbrace{\begin{bmatrix} -l_1 & 1 & 0 \\ -l_2 & 0 & 1 \\ -l_3 & 0 & 0 \end{bmatrix}}_{A-LC} \begin{bmatrix} \hat{z}_1(t) \\ \hat{z}_2(t) \\ \hat{z}_3(t) \end{bmatrix} + \begin{bmatrix} 0 \\ b \\ 0 \end{bmatrix} u(t) + \begin{bmatrix} l_1 \\ l_2 \\ l_3 \end{bmatrix} x(t) \tag{15}$$

The state feedback control law is then based on the estimate:

$$\begin{aligned} u(t) &= \frac{u_0(t) - \hat{z}_3(t)}{b_0} \\ u_0(t) &= K_p\left(r(t) - \hat{z}_1(t)\right) - K_D \hat{z}_2(t) \end{aligned} \tag{16}$$

By substituting (16) into (13), we obtain:

$$\ddot{x}(t) \approx u_0(t) = K_p\left(r(t) - x(t)\right) - K_D \dot{x}(t) \tag{17}$$

The closed-loop transfer function derived from the Laplace transform of (17) is given by:

$$G(s) = \frac{X(s)}{R(s)} = \frac{K_p}{s^2 + K_D s + K_p} \tag{18}$$

With T_{set} being the desired settling time of the system, the ADRC parameters are calculated as follows [26]:

$$\begin{cases} s^{CL} \approx \dfrac{-5.85}{T_{set}}, K_p = \left(s^{CL}\right)^2, K_D = -2s^{CL} \\ l_1 = -3s^{ESO}, l_2 = 3\left(s^{ESO}\right)^2, l_3 = -\left(s^{ESO}\right)^3 \\ s^{ESO} \approx k.s^{CL}, k > 1 \end{cases} \tag{19}$$

3.2 Model-based input filter

The input filter design method based on model reference is a design approach aimed at minimizing the difference between the actual system output and the reference model output [21].By reducing the deviation between the outputs, the input filter ensures that the actual system response follows the reference result. The general structure of the method is illustrated in Figure 4 where $F(s)$ and $G_r(s)$ are the transfer functions of the filter and the reference model, respectively.This method offers several key advantages: (a) it only requires the system output signals, and (b) it allows for selecting appropriate damping and bandwidth for the overall system to achieve the desired dynamics. Therefore, when combined with the ADRC controller, it not only effectively eliminates output vibrations but also enables the system to achieve the desired response time.

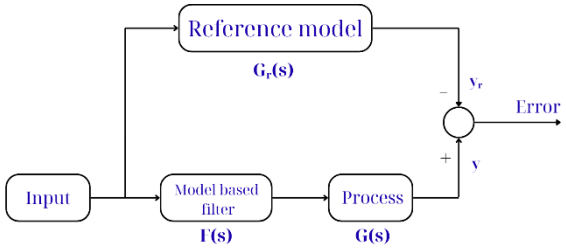

Figure 4. Model based Input filter design

Consider the plant with the following transfer func–tion:

$$G(s) = \frac{k\omega_n^2}{s^2 + 2\xi\omega_n s + \omega_n^2} \tag{20}$$

Where ξ is damping ratio, ω_{in} is natural frequency and the gain is k.The objective of designing the filter $F(s)$ is to reduce the oscillations of the plant $G(s)$. For an oscillatory plant of the above form, the transfer function of the reference model can be proposed as:

$$G_r(s) = \frac{H(s)}{s^2 + 2\xi_m\omega_m s + \omega_m^2} \tag{21}$$

In that case, the filter can be proposed in the following form:

$$F(s) = \frac{a_2 s^2 + a_1 s + a_0}{s^2 + 2\xi_m\omega_m s + \omega_m^2} \tag{22}$$

a_2, a_1, a_0 are the coefficients to be determined such that $F(s)G(s) \approx G_r(s)$. Let $y(t)$ and $y_r(t)$ denote the unit-step responses of $F(s)G(s)$ and $G_r(s)$. To achieve $F(s)G(s) \approx G_r(s)$,the difference between $y(t)$ and $y_r(t)$ should be minimized. A cost function is defined as follows:

$$E = \int_0^\infty \left(y(t) - y_r(t)\right) dt \tag{23}$$

The objective now is to determine the filter para–meters such that E is minimized. In practice, the integration interval can be chosen as a sufficiently large finite time T.

$$E = \int_0^T \left(y(t) - y_r(t)\right)^2 dt \tag{24}$$

Let $F_d(s) = s^2 + 2\zeta_{mj}\omega_{mj}s + \omega^2{}_{\text{mj}}$ and $f_i(s) = s^i/F_d$. Then we have:

$$F(s)G(s) = \sum_{i=0}^{2} a_i f_i(s) G(s) \tag{25}$$

Denote the unit-step response of $f_i(s)G(s)$ by $y_i(t)$, then:

$$y(t) = \sum_{i=0}^{2} a_i y_i(t) \tag{26}$$

Note that $y(t)$ is not determined if $F(s)$ is unknown, but the responses $y_i(t)$ can be determined once $F_d(s)$ is specified.

Substituting (26) into (24) and, by the least-squares method, the necessary and sufficient condition for E to attain its minimum is:

$$\frac{\partial E}{\partial \mathrm{a}_k} = 0, k = 0,1,2 \tag{27}$$

The values of a_0, a_1, a_2 can be obtained by solving the equations:

$$\sum_{i=0}^{2} a_i S_{k,i} - S_{k,r} = 0; k = 0,1,2 \tag{28}$$

where

$$\begin{aligned} S_{k,i} &= \int_0^T \left(y_k(t) y_i(t)\right) dt \\ S_{k,r} &= \int_0^T \left(y_k(t) y_r(t)\right) dt \end{aligned} \tag{29}$$

In practical applications, the discrete forms of $S_{k,i}$ and $S_{k,r}$ are used for the design:

$$\begin{aligned} S_{k,i} &= \sum_{j=0}^{N} \left(y_k(j\Delta t) y_i(j\Delta t)\right) \\ S_{k,r} &= \sum_{j=0}^{N} \left(y_k(j\Delta t) y_r(j\Delta t)\right) \end{aligned} \tag{30}$$

with Δt is the sampling period and $N = T/\Delta t$. Once $y_i(j\Delta t)$ and $y_r(j\Delta t)$ have been sampled, $S_{k,i}$ and $S_{k,r}$ can be computed using (30), and a_0, a_1, a_2 can then be obtained from (28).

For the crane model, since the transfer function between the payload swing angle and the trolley position is of second order, based on several experiments, this paper proposes selecting the reference transfer fun–ction for the payload swing angle $\theta(t)$ in the following form:

$$G_r(s) = \frac{-s}{\left(s + \omega_f\right)^2} \tag{31}$$

where $\lim_{s\to 0} G_r(s) = 0$ and $\lim_{s\to\infty} G_r(s) = 0$

In that case, the output-based filter is designed in the following form:

$$F(s) = \frac{a_2 s^2 + a_1 s + a_0}{\left(s + \omega_f\right)^2} \tag{32}$$

Note that when the filter is placed in front of the position controller as in the structure shown in Figure 3, the closed-loop transfer function between the reference position and the actual trolley position becomes:

$$G'_{cl}(s) = F(s) \frac{K_p}{s^2 + K_D s + K_p} \tag{33}$$

Therefore, to ensure the trolley position still tracks the reference position, we choose $a_0 = \omega^2{}_f$, in other words:

$$\lim_{s\to 0} F(s) \frac{K_p}{s^2 + K_D s + K_p} = 1 \tag{34}$$

In this case, the filter has only two parameters, a_2 and a_1, which need to be calculated based on (24). In this paper, the filter parameters are computed for $\omega_f = 2$, 4 and 6 for a comparison.

4. SIMULATION AND EXPERIMENT RESULTS

4.1 Simulation results

To verify the effectiveness of the proposed control structure for the crane system, simulations are first con–ducted using the transfer functions given in equations (10) and (11). The ADRC controller parameters for trolley position control are selected as presented in Table 1.

Table 1. ADRC Parameters

Parameter	Value	Parameter	Value
$\boldsymbol{b_0}$	100	s_{ESO}	-195
$\boldsymbol{T_{set}}$	3 (s)	l_1	585
s_{CL}	-1.95	l_2	114075
$\boldsymbol{K_p}$	3.8025	l_3	7414875
$\boldsymbol{K_D}$	3.9		

With the above parameters and the model constructed in Figure 5, simulations were performed to obtain the sampled values of $\theta_2(j\Delta t)$, $\theta_1(j\Delta t)$, $\theta_0(j\Delta t)$, $\theta_r(j\Delta t)$. Noted that:

$$f_1 = \frac{1}{\left(s + \omega_f\right)^2}, f_2 = \frac{s}{\left(s + \omega_f\right)^2} \text{ and } f_3 = \frac{s^2}{\left(s + \omega_f\right)^2},$$

Selecting $\Delta t = 0.5$s, $T = 10$s $\rightarrow N = 20$, and using (28) and (30), we computed the filter coefficients a_2, a_1, a_0 for $\omega_f = 2$, 4 and 6 as listed in Table 2.

Table 2. Model based input filter coefficients

$\omega_f = 2$	$\omega_f = 4$	$\omega_f = 6$
$a_2 = 0.1995$	$a_2 = 0.9119$	$a_2 = 2.0491$
$a_1 = 0.3483$	$a_1 = 0.2455$	$a_1 = 0.0283$
$a_0 = 4$	$a_0 = 16$	$a_0 = 36$

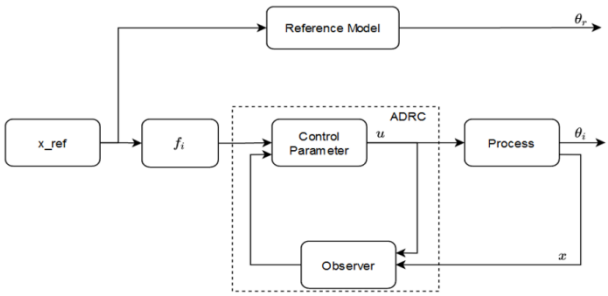

Figure 5. Filter computation model.

The simulation results are presented in Figures 6, 7 and 8. A comparative analysis of the three cases shows that each filter frequency ω_f leads to a different trade-off between swing suppression and trolley position settling time. For $\omega_f = 2$, the initial swing angle is the smallest, about 0.8° (a reduction of 2.4°compared with the case without the filter), and it decreases to around 0.2° after the trolley stops. However, the position settling time is the longest, approximately 4.35s. In contrast, for $\omega_f = 4$, the initial swing angle increases slightly to about 1.2°, with a shorter position settling time of 3.45s, and the oscillation almost completely vanishes after the trolley reaches its position. For ω_f = 6, the shortest position settling time of about 3.2s is obtained, but the initial swing angle becomes the largest, approximately 1.45°, and the oscillation disappears once the trolley achieves the desired position. These results highlight the trade-off between swing suppression and settling performance when selecting the filter frequency.

Regarding the control input voltage, the original ADRC produces the largest peak amplitude of 4.5 V. In contrast, the ADRC with filter significantly reduces the input peak, especially with $\omega_f = 2$, where the maximum voltage is limited to around 2.6 V. Although this reduction results in smoother and less demanding con–trol signals, it also introduces a slower position res–ponse. The cases with ω_f = 4 and ω_f = 6 provide intermediate performance, where the control input is moderated while maintaining a relatively fast system response. Importantly, all control input values remain within the expected operating range of −10 V to 10 V, ensuring the practicality of implementation in experi–ment system.

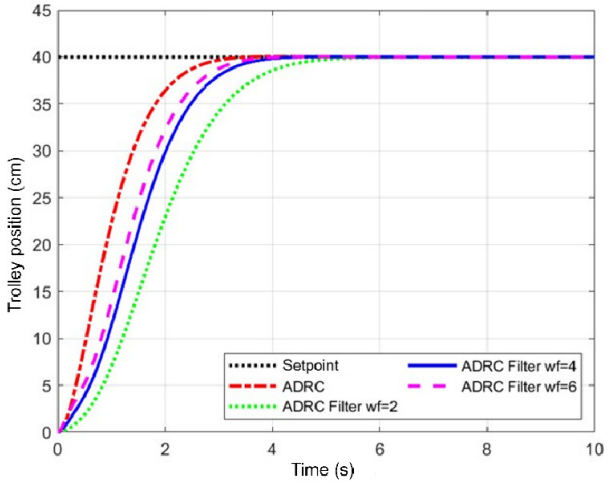

Figure 6. Simulationtrolley position response

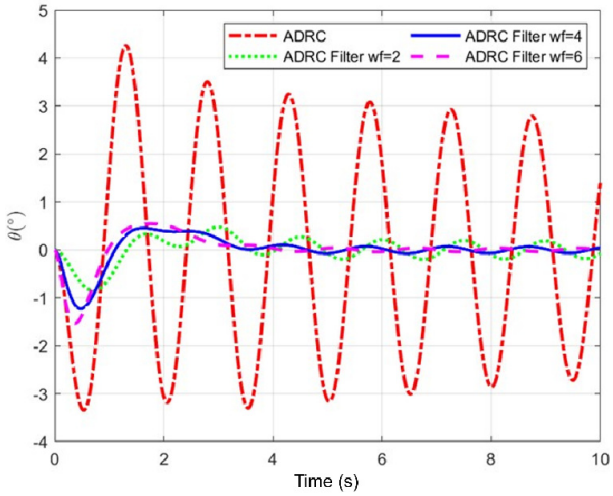

Figure 7. Simulation payload sway angle response

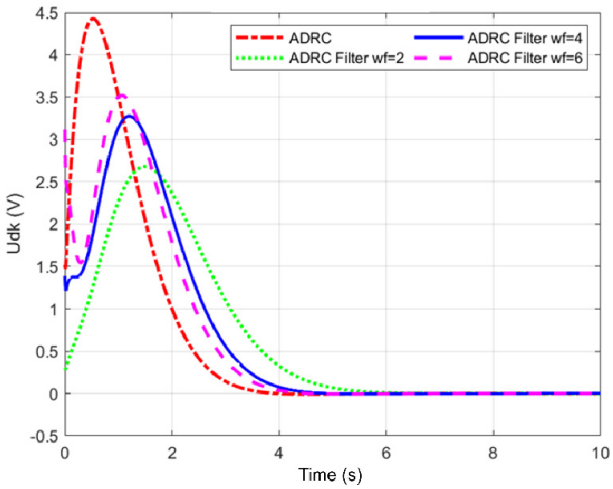

Figure 8. Simulationinput voltage

4.2 Experiment validation

For the experiment implementation, the ADRC and filter parameters are selected to be the same as those used in the simulation, as presented in Tables1 and 2. Two scenarios are considered.

Scenario 1: in this experiment, the trolley is controlled to move a distance of x = 40 cm with a rope length of l = 1 m and a payload mass of m = 1 kg. The results are shown in Figure 9 to 13.

The experiment results validate the effectiveness of the proposed control scheme with the integration of the designed input filter. Specifically, when the filter para–meter was set to $\omega_f = 2$, the trolley motion exhibited the smallest initial swing angle, approximately 1.2°, which corresponds to a reduction of around 2° compared to the case without filter. The residual oscillation after the trolley reached its final position was about 0.4°. Nevertheless, this configuration resulted in the longest position settling time of approximately 4.26 s, significantly longer than the time 2.5 s observed without filtering. When the filter was tuned to $\omega_f = 4$, the system achieved a faster response with a settling time of about 3.25 s. The initial swing angle was slightly higher at around 1.4°, but the oscillation diminished almost completely once the trolley settled, indicating an improved balance between swing suppression and

positioning speed. Increasing the filter frequency to ω_f = 6 resulted in the shortest settling time of approximately 3 s. However, this advantage came at the expense of a larger initial swing angle of about 1.85°, corresponding to only a 1.4° reduction, before eventually decaying after the trolley reached the desired position.

Across all experimental conditions, the control input voltage remained well within the expected operating range of −10 V to 10 V, confirming that the controller operates safely within the signal input limitations. This aspect highlights the practical feasibility of implementing the proposed method. A comparative analysis between experimental and simulation also demonstrates strong consistency in both position response and swing behavior. Minor differences between the simulation and experiment results can be attributed to unavoidable disturbances in the experimental environment and parameter approximation during simulation.

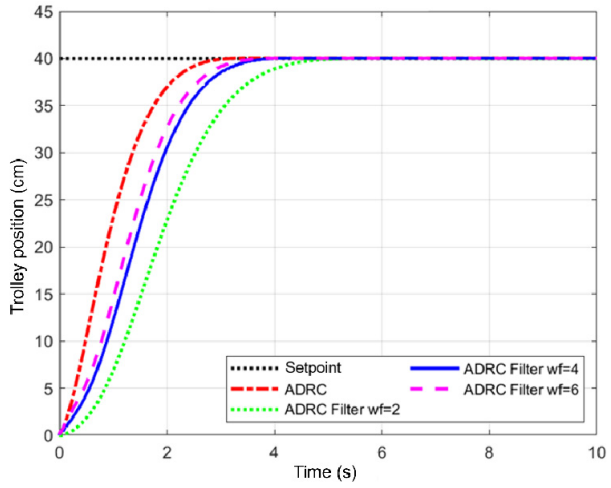

Figure 9. Experimenttrolley position response

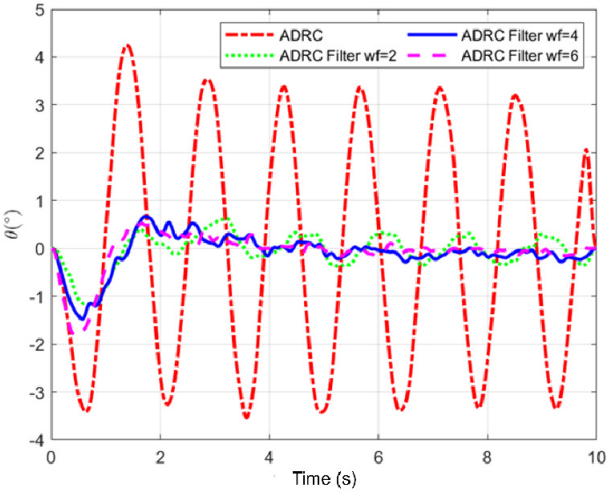

Figure 10. Experiment payload sway angle response

Overall, the case with ω_f = 4 can be regarded as the most favorable choice, since it achieves a satisfactory compromise between fast trolley positioning and effective swing suppression. These findings not only reinforce the robustness of the proposed controller but also demonstrate that careful tuning of the filter parameter ω_f is critical in optimizing the trade-off between positioning performance and oscillation reduction in practical applications.

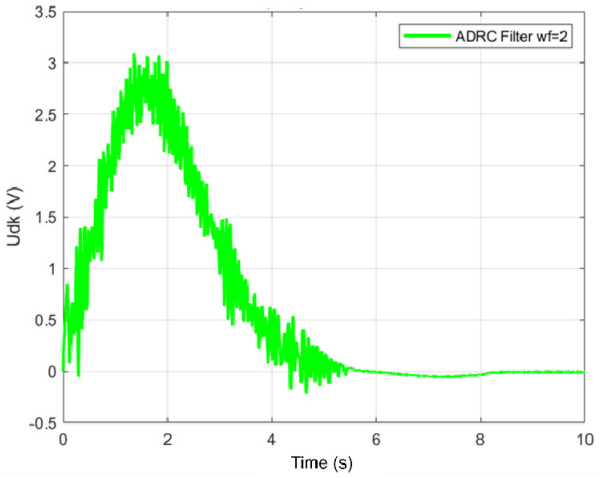

Figure 11. Control input voltage for ω_f = 2

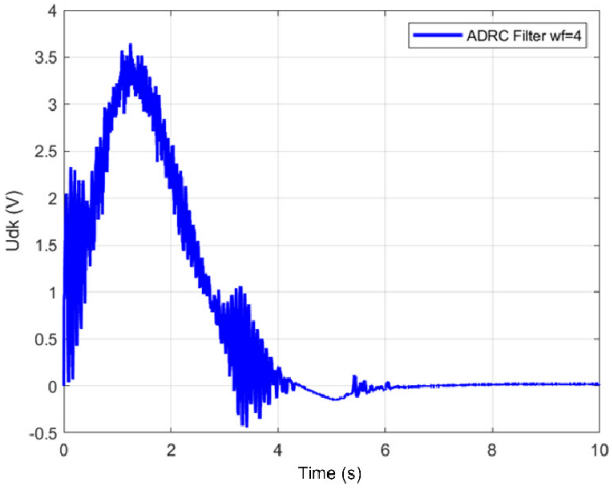

Figure 12. Control input voltage for ω_f = 4

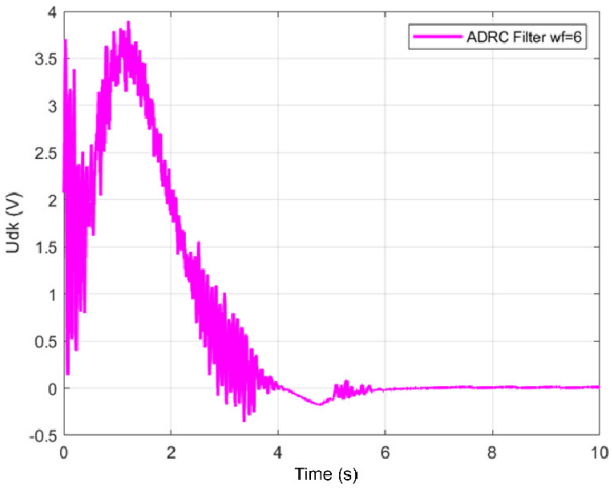

Figure 13. Control input voltage for ω_f = 6

Scenario 2: In this scenario, the robustness of the proposed control method is evaluated. The ADRC controller parameters are kept unchanged, as presented in Table 1, while the filter parameter is fixed at ω_f = 4 according to Table 2. Two cases are investigated sequentially: variation of the payload mass andvariation of the rope length. These tests aim to examine the controller's ability to maintain satisfactory performance under parameter uncertainties and operating condition changes.

When the payload mass varies from 0.6 kg to 2.2 kg, as can be seen in Figure 14 to Figure 17, the proposed control scheme consistently maintains accurate position tracking, with the settling time remaining nearly unchanged compared to the nominal case of 1 kg. This is a significant advantage, demonstrating the robustness and adaptability of the control structure to payload variations. The disturbance rejection mechanism of ADRC allows the system to automatically adjust the control effort to ensure the desired response, thereby preventing the increase in settling time even when the payload mass is significantly higher.Regarding payload oscillations, the integrated filter plays a crucial role in suppressing the initial swing amplitude. Specifically, for the 2.2 kg payload, the initial swing angle is reduced from 3.2° (ADRC without filter) to 1.2° (ADRC with filter), and the oscillation almost vanishes once the trolley reaches the target position. Similarly, for the 0.6 kg payload, the initial swing angle decreases to 1.1°. These results highlight the importance of the filtering mechanism in mitigating load oscillations, which are a major source of instability and safety concerns in crane operations.

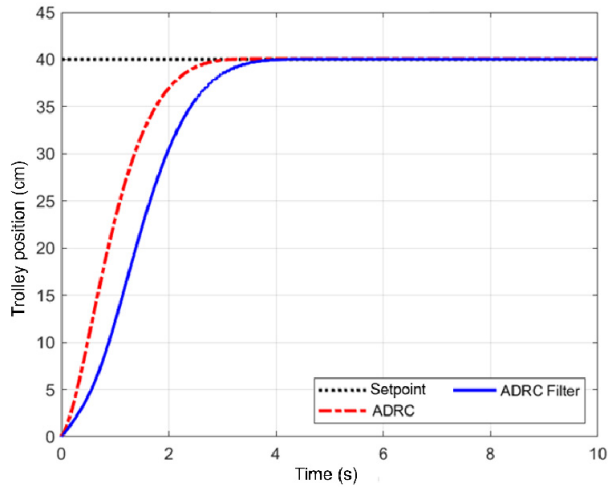

Figure 14. Trolleyposition response when m_P=2.2 kg

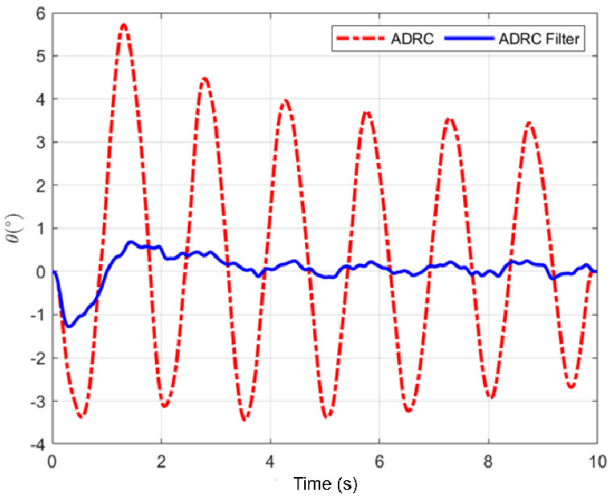

Figure 15. Payload sway angle response when m_P=2.2 kg

As illustrated in Figure 18 to Figure 21 , changing the cable length does not significantly affect the position settling time, which remains almost constant under different conditions. However, the influence of the filter on suppressing payload oscillations is clearly observed. When the rope length is shortened to l = 0.45 m, the filter reduces the initial swing amplitude from 3.8° to 1.2°, and the oscillation decreases to about 0.3° when the trolley reaches the target position. Conversely, when the rope length is increased to l = 0.65 m, the filter lowers the initial swing from 3.1° to 1.1°, and the residual oscillation at steady state is approximately 0.2°.

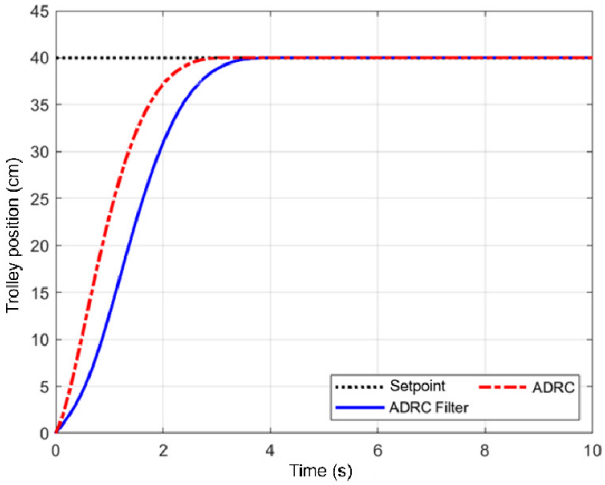

Figure 16. Trolleyposition response when m_P=0.6 kg

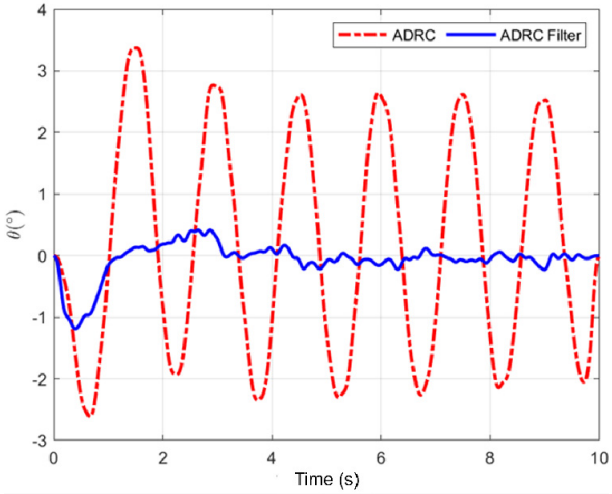

Figure 17. Payload sway angle response when m_P=0.6 kg

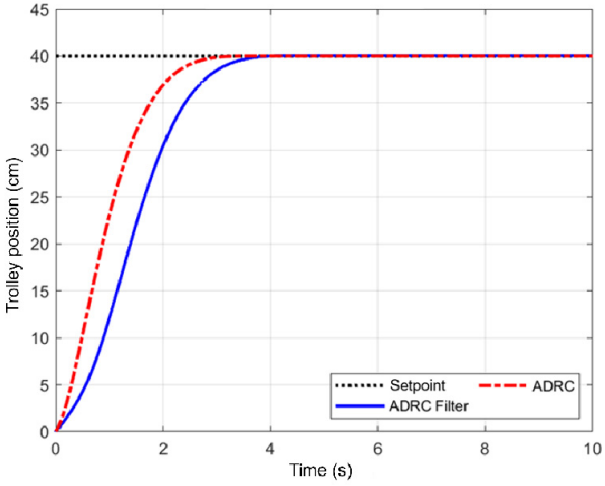

Figure 18. Trolleyposition response when l = 0.45 m

These results confirm that the filter consistently improves swing suppression across different rope lengths while preserving the fast and stable position res–ponse ensured by ADRC. This robustness is particularly important for overhead cranes, where rope length frequently changes during operation, and uncontrolled oscillations can compromise both efficiency and safety.

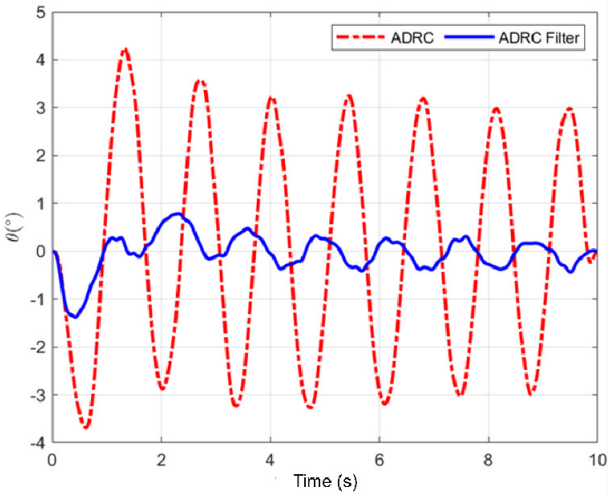

Figure 19. Payload sway angle response when l = 0.45 m

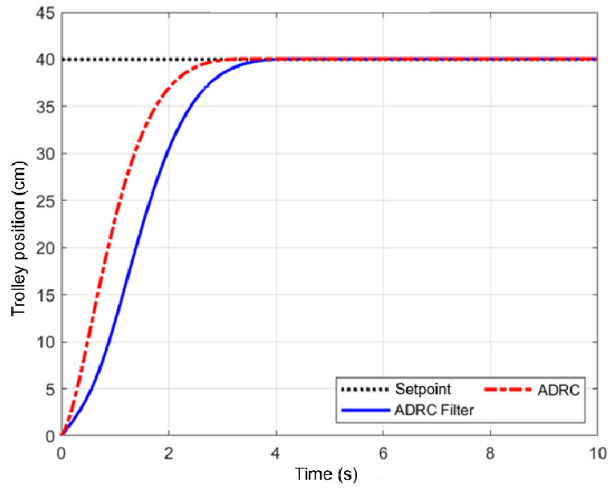

Figure 20. Trolleyposition response when l = 0.65 m

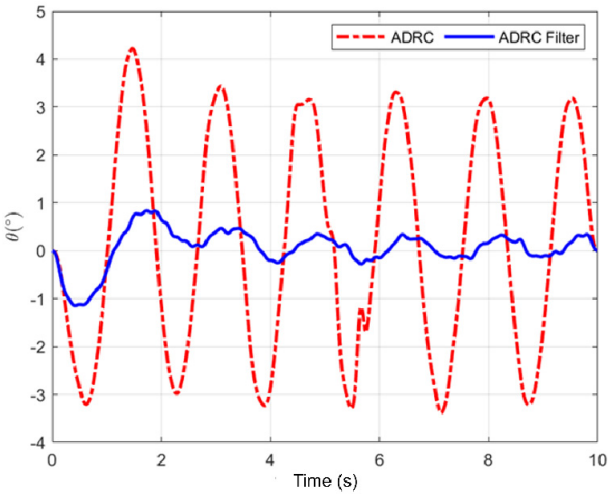

Figure 21. Payload sway angle response when l = 0.65 m

Overall, the results demonstrate the effectiveness of the proposed control strategy in ensuring both fast and stable position response while substantially reducing payload oscillations, even under significant variations in payload mass.

5. CONCLUSIONS

This paper has proposed a hybrid control framework that integrates Active Disturbance Rejection Control (ADRC) with a model-based input filter for the position regulation and oscillation suppression of an overhead crane system. A key advantage of the proposed design is that it requires only system output measurements, thereby reducing the dependency on detailed system modeling, which is often difficult to obtain in practical crane operations. Simulation studies have demonstrated that the method achieves accurate trolley positioning while effectively attenuating payload oscillations. Furthermore, robustness analyses under variations in rope length and payload mass confirm that the proposed approach maintains reliable performance across dif–ferent operating conditions. These findings highlight the potential of the proposed hybrid scheme as a practical and effective solution for overhead crane control, ensuring both high efficiency and improved safety.

ACKNOWLEDGMENT

The author would like to thank Mr. Anh Dung Tran for his assistance with the experimental setup.

REFERENCES

[1] Singhose, W. E., Lawrence, J., Sorensen, K. L., Dooroo, K., Applications and educational uses of crane oscillation control, FME Transactions, 34:175–183, 2006.

[2] Mojallizadeh, M. R.,Brogliato, B., Prieur, C.: Mo–deling and control of overhead cranes: A tutorial overview and perspectives, Annual Reviews in Control, 56:100877, 2023.

[3] Jaafar, H.I., Hussien, S.Y.S., Ghazali, R., Mohamed, Z: Optimal tuning of PID+PD controller by PFS for Gantry Crane System, 2015 10th Asian Control Conference (ASCC), Kota Kinabalu, Malaysia, 2015, pp. 1-6.

[4] Sun, Z., Wang, N., Bi Y., and Zhao J.: A DE based PID controller for two dimensional overhead crane, 2015 34th Chinese Control Conference (CCC), Hangzhou, China, 2015, pp. 2546-2550.

[5] Sun, N., Yang, T., Fang, Y., Wu, Y., Chen, H.: Transportation control of double-pendulum cranes with a nonlinear quasi-pid scheme: Design and experiments, IEEE Transactions on Systems, Man, and Cybernetics: Systems, 49(7):1408–1418, 2019.

[6] Wang, X. J., Chen, Z. M.: Two-degree-of-freedom sliding mode anti-swing and positioning controller for overhead cranes, 2016 Chinese Control and Decision Conference (CCDC), Yinchuan, China, 2016, pp. 673-677.

[7] Park, M. -S, Chwa, D. ,Eom, M.: Adaptive Sliding-Mode Antisway Control of Uncertain Overhead Cranes With High-Speed Hoisting Motion, IEEE

Transactions on Fuzzy Systems, vol. 22, no. 5, pp. 1262-1271, Oct. 2014.

[8] Akira, A.: Non-linear control technique of a pendu–lum via cable length manipulation: Application of particle swarm optimization to controller design, FME Transactions, 41:265–270, 2013.

[9] Chen, H., Fang, Y., Sun, N.: A swing constraint guaranteed mpc algorithm for under actuated overhead cranes. IEEE/ASME Transactions on Mechatronics, 21(5):2543–2555, 2016.

[10] Zhang, Z., Wu, Y., Huang, J.: Differential flatness-based finite-time anti-swing control of under actuated crane systems, Nonlinear Dynamics, 87, 02 2017.

[11] Chang, C. Y.: Adaptive Fuzzy Controller of the Overhead Cranes with Nonlinear Disturbance, IEEE Transactions on Industrial Informatics, vol. 3, no. 2, pp. 164-172, May 2007.

[12] Singer, N. C., Seering, W. P.: Preshaping command inputs to reduce system vibration, Journal of Dy–namic Systems, Measurement, and Control, 112(1):76–82, 03 1990.

[13] Singhose, W., Seering, W., Singer, N.: Residual Vibration Reduction Using Vector Diagrams to Generate Shaped Inputs, ASME Journal of Dynamic Systems, Measurement, and Control, 116, 654-659, 1994.

[14] Wahrburg, A., Jurvanen, J., Niemela, M., Holmberg, M.: Input shaping for non-zero initial conditions and arbitrary input signals with an application to overhead crane control,in 2022 IEEE 17th Inter–national Conference on Advanced Motion Control (AMC), pages 36–41. IEEE, 2022.

[15] Abdullah Mohammed, A., Alghanim, K. and Taheri Andani, M.: An adjustable zero vibration input shaping control scheme for overhead crane systems, Shock and Vibration, 2020(1):7879839.

[16] Huey, J. R.: The intelligent combination of input shaping and PID feedback control," PhD diss., Georgia Institute of Technology, 2006.

[17] Do, T. H., Duong, M. D., Nguyen, M. L., Dao, Q. T.: A Combination of Distributed Delays Shapers and ADRC for Gantry Crane Control, 2020 Inter–national Conference on Advanced Mechatronic Systems (ICAMechS), Hanoi, Vietnam, 2020, pp. 124-128.

[18] Tong, T. L., Nguyen, D. C., Duong, M. D.: Integrating Active Disturbance Rejection Control and Input Shaping for Enhanced Vibration Control of Warehouse Single Mast Stacker Crane, Journal of Applied Science and Engineering, 28(11): 2391-2399, 2025.

[19] Do, T. H., Nguyen, M. D., Duong, M. D.: A Modified ETM Shaper for Double Pendulum Crane Control with Payload hoisting, Journal of Applied Science and Engineering, 28(8): 1727-1735, 2024.

[20] Han, J.: From pid to active disturbance rejection control, IEEE Transactions on Industrial Elect–ronics, 56(3):900–906, 2009.

[21] Han, J., Zhu, Z., He Y., Qi, J.: A novel input sha–ping method based on system output, Journal of Sound and Vibration, Volume 335, pp. 338-349, 2015.

[22] Solihin, M. I., Wahyudi, Legowo, A.: Fuzzy-tuned PID Anti-swing Control of Automatic Gantry Crane, Journal of Vibration and Control 16(1): 127–145, 2010.

[23] Trinh, M. C., Do, T. H, Dao, Q. T.: Development of a Rehabilitation Robot: Modeling and Trajectory Tracking Control, ASEAN Engineering Journal 12(4): 121–129, 2022.

[24] Tong, T. L., Nguyen, T. A., Duong, M. D.: Flatness -Based Linear Active Disturbance Rejection Con–trol for Tower Crane, FME Transactions, 53(2): 363–371, 2025.

[25] Herbst, G.: A Simulative Study on Active Distur–bance Rejection Control (ADRC) as a Control Tool for Practitioners, Electronics, 2(3):246–279, 2013.

[26] Nguyen, V. D., Duong, M. D., Do, T. H.: Enhanced overhead crane control using ADRC and ZVD input shaping with trajectory planning, FME Transactions, 53(3):363–371, 2025.

NOMENCLATURE

x	trolley position
l	cable length
θ	sway angle of the payload
m_t	trolley mass
m_p	payload mass
B_{eq}	damping coefficient along the x-axis
B_p	rotational damping coefficient
T_{set}	2% settling time

Greek symbols

ξ	damping ratio
ω_n	natural frequency

Acronyms and Abbreviations

ADRC	Active Disturbance Rejection Control
ESO	Extended State Observer

КОМБИНОВАНИ УЛАЗНИ ФИЛТЕР ЗА АДРЦ И РЕФЕРЕНТНИ МОДЕЛ ЗА КОНТРОЛУ НАДЗЕМНЕ ДИЗАЛИЦЕ: ДИЗАЈН И ЕКСПЕРИМЕНТАЛНА ВАЛИДАЦИЈА

Т. Х. До

Мостне дизалице се широко користе у индустрији и транспорту, али на њихов рад често утичу нежељене осцилације корисног терета које деградирају управљивост и сигурност. Иако су истражене бројне стратегије управљања, већина њих је релативно сложена како у дизајну контролера тако иу практичној имплементацији. Овај рад предлаже хибридну контролну шему која интегрише Ацтиве Дистурбанце Рејецтион Цонтрол (АДРЦ) са улазним филтером заснованим на референци модела, где

АДРЦ обезбеђује тачно позиционирање колица и филтер потискује промене корисног оптерећења .смањујући потребу за прецизним моделирањем система и ублажавајући утицај несигурности параметара. Резултати симулације потврђују да предложени приступ ефикасно елиминише осцилације корисног терета уз постизање жељеног позиционирања, а експерименталне валидације додатно демонстрирају његову робусност и практичну изводљивост за операције дизалица.